Biochemical Pharmacology 80 (2010) 1466–1477

Contents lists available at ScienceDirect

Biochemical Pharmacology

journal homepage: www.elsevier.com/locate/biochempharm

Doxorubicin-induced cell death requires cathepsin B in HeLa cells

S. Bien [a], C. Rimmbach [a], H. Neumann [a], J. Niessen [a], E. Reimer [a], C.A. Ritter [a], D. Rosskopf [a], J. Cinatl [c], M. Michaelis [c], H.W.S. Schroeder [b], H.K. Kroemer [a,*]

[a] Department of Pharmacology, Ernst Moritz Arndt University, Friedrich Loefflerstr. 23d, 17487 Greifswald, Germany
[b] Clinic of Neurosurgery, Ernst Moritz Arndt University, Greifswald, Germany
[c] Institute of Medical Virology, Clinics of the Goethe-University, Frankfurt am Main, Germany

ARTICLE INFO

Article history:
Received 14 May 2010
Accepted 27 July 2010

Keywords:
Doxorubicin
Cathepsin B
Cell death

ABSTRACT

The cysteine protease cathepsin B acts as a key player in apoptosis. Cathepsin B-mediated cell death is induced by various stimuli such as ischemia, bile acids or TNFα. Whether cathepsin B can be influenced by anticancer drugs, however, has not been studied in detail. Here, we describe the modulation of doxorubicin-induced cell death by silencing of cathepsin B expression. Previously, it was shown that doxorubicin, in contrast to other drugs, selectively regulates expression and activity of cathepsin B.

Selective silencing of cathepsin B by siRNA or the cathepsin B specific inhibitor CA074Me modified doxorubicin-mediated cell death in Hela tumor cells. Both Caspase 3 activation and PARP cleavage were significantly reduced in cells lacking cathepsin B. Moreover, mitochondrial membrane permeabilization as well as the release of cytochrome C and AIF from mitochondria into cytosol induced by doxorubicin were significantly diminished in cathepsin B suppressed cells. In addition, doxorubicin associated down-regulation of XIAP was not observed in cathepsin B silenced cells. Lack of cathepsin B significantly modified cell cycle regulatory proteins such as cdk1, Wee1 and p21 without significant changes in G_1, S or G_2M cell cycle phases maybe indicating further cell cycle independent actions of these proteins. Consequently, cell viability following doxorubicin was significantly elevated in cells with cathepsin B silencing.

In summary, our data strongly suggest a role of cathepsin B in doxorubicin-induced cell death. Therefore, increased expression of cathepsin B in various types of cancer can modify susceptibility towards doxorubicin.

1. Introduction

Most anticancer drugs trigger cell death through apoptosis or activate a program leading to growth arrest. The underlying molecular pathways have been thoroughly characterized for several substances. Among them, cathepsin B has been of particular interest. In fact, cathepsin B is a crucial component in different models of apoptosis including neuronal apoptosis [1], or bile acid-induced hepatocyte apoptosis [2]. Furthermore, hepatocytes from cathepsin B knockout mice are resistant to TNFα-induced apoptosis [3]. Similarly, TRAIL-induced apoptosis of oral cancer cells is also mediated by cathepsin B [4] and induction of this protease upon 1,25-dihydroxy vitamin D(3) is accompanied by sensibilization of tumor cells against TNFα [5]. Furthermore, inhibition of cathepsin B significantly reduces hepatocyte apoptosis and liver injury in cholestasis [6] or TNFα-induced acute liver failure [3]. Finally, cathepsin B expression is significantly elevated in various types of cancer [7] suggesting this protease as a suitable drug target. However, the role of this cysteine protease for cell death induced by anticancer drugs has not been addressed in detail. Recent evidence using pharmacological inhibition of cathepsin B points to a role of this protease in proteasome inhibitor PS-341 (bortezomib) [8] and paclitaxel induced cell death [9] but only slightly in camptothecin mediated apoptosis [10] suggesting a stimuli dependent involvement of cathepsin B.

Testing a variety of anticancer drugs, we could recently demonstrate a selective regulation of cathepsin B expression and activity by doxorubicin suggesting that this protease could be involved in doxorubicin-mediated cell death [11]. Doxorubicin is one of the most important anticancer drugs used in a wide variety of malignancies including breast cancer, cervix carcinoma or lymphoma [12,13]. Despite its longstanding clinical use, the antiproliferative and death-inducing action of doxorubicin remains controversially discussed. Proposed modes of action involve intercalation into DNA, inhibition of topoisomerase II, free radical generation and damage of cell membrane permeability and fluidity [14] triggering tumor cell death [15] in which caspases are considered to be major executioners. Blocking caspase activation did not prevent cell killing in leukemic blast cells and neuroblastoma cells induced by chemotherapeutics including doxorubicin [16,17]. Additionally,

* Corresponding author. Tel.: +49 3834 865630; fax: +49 3834 865631.
E-mail address: kroemer@uni-greifswald.de (H.K. Kroemer).

0006-2952/$ – see front matter © 2010 Elsevier Inc. All rights reserved.
doi:10.1016/j.bcp.2010.07.036

doxorubicin-induced death in neuroblastoma cells is also caspase-independent [18] and caspase inhibition switches doxorubicin-induced apoptosis to senescence [17]. These data strongly suggest that additional factors play a pivotal role in cell death.

In this paper, we identify a significant contribution of cathepsin B to doxorubicin-induced cell death and characterized the molecular mechanisms. Using siRNA technology we demonstrate reduced Caspase 3 activation and PARP cleavage, decreased loss of mitochondrial membrane permeabilization and release of cytochrome C and AIF into cytosol in doxorubicin-treated cathepsin B silenced cells. Distinct regulation of apoptotic and cell cycle regulatory proteins in cathepsin B suppressed cells was accompanied by a reduction in subG$_1$ fraction. A lack of significant changes in the other cell cycle phases, however, may be indicative of additional cell cycle independent actions of the regulated proteins.

In summary, our data provide evidence for cathepsin B dependent modulation of doxorubicin-induced cell death.

2. Materials and methods

2.1. Materials

Doxorubicin hydrochloride (Sigma–Aldrich, Deisenhofen, Germany) stock solutions were prepared in dimethyl sulfoxide (DMSO). Trypsin, RPMI1640 and DMEM were from PAN (Aidenbach, Germany). FCS and Lysotracker Red were obtained from Invitrogen (Karlsruhe, Germany). The cathepsin B specific inhibitor CA-074Me, the cathepsin B substrate Z-AMC and propidium iodide were from Sigma–Aldrich (Deisenhofen, Germany).

2.2. Cell lines, culture conditions and retroviral infection

HeLa cells were cultured in RPMI1640 supplemented with 10% FCS, 2 mM glutamine, 100 U/ml penicillin and 100 μg/ml streptomycin at 37 °C under 5% CO_2.

Further cell lines used for this study were the glioma cell lines U87-MG and LN18, the hepatoma cell line HepG2, the pancreatic adenocarcinoma cell line PaTuO2, the colon carcinoma cell line Caco2 (all cell lines were obtained from ATCC, Manassas, VA, USA). Additionally, we tested a panel of parental doxorubicin-sensitive and doxorubicin-resistant cell lines. The neuroblastoma cell line UKF-NB-3 was established from bone marrow metastasis of an own patient (Kotchetkov et al. [19]). IMR-32 neuroblastoma cells and H9 lymphoma cells were obtained from ATCC (Manassass, VA, USA). The rhabdomyosarcoma cell line HA-OH1 was kindly provided by Dr. Koscielniak (Olgahospital Stuttgart, Germany). The Ewing's sarcoma cell line MHH-ES-1, the osteosarcoma cell line SAOS-2, and the bladder cancer cell line TCC-SUP were received from DSMZ (Braunschweig, Germany). The prostate cancer cell line DU145 was obtained from DKFZ (Heidelberg, Germany). Cells were adapted to growth in the presence of doxorubicin (DOX, obtained from medac Gesellschaft für klinische Spezialpräparate mbH, Hamburg, Germany) by described methods and named following the published nomenclature [19], i.e. UKF-NB-3^{r}DOX^{20} means UKF-NB-3 adapted to growth in the presence of doxorubicin 20 ng/ml resulting in the following sub-lines: HA-OH1^{r}DOX^{20}, IMR-32^{r}DOX^{10}, MHH-ES-1^{r}DOX^{50}, SAOS-2^{r}DOX^{20}, TCC-SUP^{r}DOX^{100}, H9^{r}DOX^{20}. All cell lines were grown in IMDM supplemented with 10% FCS, 100 IU/ml penicillin, and 100 mg/ml streptomycin at 37 °C. All cell culture materials were purchased from PromoCell GmbH (Heidelberg, Germany).

RNA sequences against cathepsin B for RNA interference were designed using *Dharmacon website siRNA design center* (http://design.dharmacon.com/rnadesign/default.aspx). The following two cathepsin B siRNA sequences (underlined) were used: cat B-1 Forward 5′-*CG AACCC*GTGGACATGAGCTACTTGA*TTCAAGAGA*GATCAAGTAGCTCATGTCCAC*TTTTTGGAAC*-3′, cat B-1 Reverse 5′-*TCGAG TTCCAAAAA*GTGGACATGAGCTACTTGA *TCTCTTGAA*TCAAGTAGCTCATGTCCAC*GGGTT*-3′, cat B-2 Forward 5′-*CGAACCCG* ACAAGCACTACGGATACA*TTCAAGAGA*TGTATCCGTAGTGCTTGTC*TTTTTGGAAC*-3′ and cat B-2 Reverse 5′-*TCGAGTTCCAAAAA*GACAAGCACTACGGATACA*TCTCTTGAA* TGTATCCGTAGTGCTTGTC*GGGTT*-3′. Annealing of the forward and reverse primer was performed using 3 μg of each oligonucleotide in 50 μl annealing buffer (100 mM NaCl, 50 mM HEPES, pH 7.4) Annealed siRNA was ligated into XhoI and Bsp119I digested retroviral vector pQCXIH (Clontech, Saint-Germain-en-Laye, France). Virus production was performed according to a standard protocol from clontech. For the inward transfer of the siRNA, HeLa cells were stably infected with empty (HeLa-Co) or cathepsin B siRNA encoding retrovirus (HeLa-cat B-2). Stably transfected sublines were generated by hygromycin (Invitrogen, Karlsruhe, Germany) selection (0.2 mg/ml).

2.3. Quantitation of cathepsin B mRNA

Quantitation of cathepsin B expression was performed by real-time polymerase chain reaction (RT-PCR). Total RNA was isolated using peqGold RNAPure (peqlab, Erlangen, Germany) and reversely transcribed with *TaqMan® Reverse Transcription Reagents* according to the manufacturer's instruction (Applied Biosystems, Weiterstadt, Germany). RT-PCR was performed with the ABI PRISM 7700 sequence detection system and was analyzed with the 1.7 software (Applied Biosystems, Weiterstadt, Germany). The cathepsin B cDNA fragment was amplified using the primers CatB-For 5′-TGGACAAGAA AAGGCCTGGTT-3′ and CatB-Rev 5′-CCGTTGACG TGGTGCTCA-3′. The sequence of the 5-carboxyfluorescein-labeled probe was 5′-CCCATGTAGGGTGCA-GACCGTACTCC-3′. Amplification of the endogenous control was performed with the ribosomal *18S Taqman PCR master mix* (Applied Biosystems, Weiterstadt, Germany). Gene expression was quantified using the threshold PCR cycle number (Ct) method ($\Delta\Delta C_T$-method).

2.4. Protein isolation and Western blotting

Cells were lysed for 30 min on ice in 50 mM Tris–HCl, 100 mM NaCl, 0.1% Triton-X100 and 5 mM EDTA (pH 7.4) supplemented with protease inhibitors (1 mM PMSF, 1 mM leupeptin, 1 mM aprotinin and 250 μg/ml sodium vanadate) and centrifuged at 13,000 × *g* for 5 min to remove cell debris. The amount of protein was determined by the BCA method using bovine serum albumine. 50 μg of protein were separated on a 12.5% SDS-PAGE and transferred to polyvinylidene fluoride membranes (Millipore). The following primary antibodies were used: anti-cathepsin B (Ab-2, Calbiochem, Darmstadt, Germany), anti-cathepsin D (E-7), anti-cathepsin L (H-80), anti-caspase 1 (A-19), anti-Bax (B-9), anti-Bcl-2 (C-2), anti-Bcl-xL (H-5), anti-PARP (F-2), anti-p21 (F-5), anti-p53, anti-Myt1 (N-17), anti-phospho-Myt1 (Ser83), anti-Wee1 (H-300), anti-cdc2 (H-297), anti-phospho-cdc2 (Thr14/Tyr15) (Santa Cruz Biotech, Heidelberg, Germany), anti-phospho-cdc25 (Ser16), anti-Bid (Cell Signalling Technology, Frankfurt am Main, Germany), anti-XIAP (BD Biosciences) and anti-glyceraldehyde-3-phosphate dehydrogenase (GAPDH, Biodesign Int., clone 6C5, Saco, Maine USA). Reactive bands were detected using enhanced chemiluminescence on X-ray films, normalized to GAPDH using Image Quant 5.0 software and shown as arbitrary units (AU).

2.5. Cathepsin activity assay

Enzyme activity of cathepsin B was determined using the specific fluorogenic substrate Z-AMC (Sigma–Aldrich, Deisenhofen, Germany) as described previously [11].

2.6. Caspase activity assays

Caspase 3, 8 and 9 activities were measured in cell lysates with commercially available Colorimetric assay kits (R&D Systems, Wiesbaden, Germany) according to the manufacturer's instructions, normalized to the respective protein content and are shown as *x*-fold increase relative to DMSO control.

2.7. Analysis of mitochondrial depolarization

FACS analysis was performed for quantification of mitochondrial membrane potential dissipitation ($\Delta\Psi_m$) using tetramethylrhodamine ethyl ester (TMRE, Molecular probes, Invitrogen, Karlsruhe, Germany). After incubation of HeLa cells with doxorubicin, cells were loaded with TMRE for 20 min at 37 °C. Thereafter, floating cells were collected by centrifugation, combined with trypsinized attached cells and analyzed by FACS at the FL-2 channel using Becton Dickinson FACSCalibur (Heidelberg, Germany). Data were expressed as percentage of intact mitochondrial membrane potential.

2.8. Release of cytochrome C and AIF into cytosol

For determination of release of cytochrome C and AIF into cytosol, cells were harvested, centrifuged at 6000 rpm for 5 min and lysed by incubating in digitonin lysis buffer (80 mM KCl, 8 mM Na_2HPO_4, 1 mM NaH_2PO_4, 1 mM EDTA, and 0.02% digitonin) for 10 min at room temperature. The lysate was centrifuged at 1000 × *g* for 10 min. The supernatant was collected and further centrifuged at 50.000 × *g* for 1 h at 4 °C. The resulting supernatant was considered as cytosolic fraction, was quantified by the BCA method and 30 μg protein were subjected to immunoblot analysis using anti-AIF (Cell Signaling Technology, Frankfurt am Main, Germany) and anti-cytochrome C (BD Pharmingen, Heidelberg, Germany). Additionally, the purity of cytosolic fraction was determined using an antibody against a mitochondria-specific protein namely Antioxidant protein 1 (not shown).

2.9. Cell cycle analysis

Determination of cell cycle was performed using propidium iodide staining. Briefly, treated and untreated cells were harvested and pooled with the floating cells. After centrifugation at 3000 rpm for 5 min, cells were washed once with PBS and fixed in ethanol overnight at 4 °C. After fixation, cells were centrifuged at 4000 rpm for 2 min and washed two times with PBS. Pellets were resuspended in 500 μl staining buffer (1% glucose, 2 mg/ml RNase A, 50 μg/ml propidium iodide) and incubated for 30 min at room temperature in the dark. Measurement of propidium iodide incorporation into DNA was analyzed by FACS at the FL-2 channel and the respective cell cycle phase was expressed as percentage of total cell population.

2.10. Cell viability assay

HeLa cells were seeded at 5000 cells/well in a 96-well multiplate. The growth medium was changed after 1 day and replaced by DMSO or doxorubicin containing media. After the respective incubation period, 1/10 of Alamar Blue (BioSource/Invitrogen, Karlsruhe, Germany) was added and analysis was performed according to the manufacturer's instruction. Data were expressed as percentage of cell viability of DMSO treated control cells.

2.11. Statistical analysis

Data represent at least three independent experiments and were expressed as the mean ± SD. Statistical analysis of data comparisons of control transfected cells with cathepsin B silenced cells was performed with Microsoft Windows XP Professional Version 2002 using Student's *t*-test and with Graph Pad Prism 5.0 using one-way ANOVA (comparison between more than two groups). Additionally, Graph Pad Prism 5.0 with nonlinear regression and Wilcoxon Signed Rank test was used for determination of IC_{50} values and comparison between control transfectants and cathepsin B suppressed cells. Correlation of IC_{50} values with cathepsin B protein expression was analyzed by Spearman's nonparametric correlation, and comparison of doxorubicin sensitive and resistant cells was performed with paired *t*-test using Graph Pad Prism 5.0. Statistical significance was defined as *p*-value < 0.05 ($^*<0.05$, $^{**}<0.01$ and $^{***}<0.001$).

3. Results

3.1. Influence of doxorubicin on cathepsin B, D and L protein expression

A time- and dose-dependent induction of cathepsin B expression by doxorubicin was demonstrated recently by our group [11] but other cathepsins potentially relevant for apoptosis were not investigated. Therefore, at first we determined the influence of doxorubicin on expression of two further cathepsins namely cathepsin D and L. Immunoblot analysis revealed no significant regulation of cathepsin D (AU DMSO 0.22 ± 0.7 and Dox 0.36 ± 0.03, $p = 0.057$) and cathepsin L (AU DMSO 0.46 ± 0.17 and Dox 0.33 ± 0.15, $p = 0.376$) upon doxorubicin in contrast to the strong induction of cathepsin B (AU DMSO 0.03 ± 0.03 and Dox 0.50 ± 0.15 after 48 h (Fig. 1A-left + right)).

3.2. Analysis of cathepsin B expression after retroviral siRNA transfection

Validation of cathepsin B suppression by retroviral siRNA transfection was performed by RT-PCR, immunoblotting and Z-AMC activity assay all representing a clear down-regulation of cathepsin B in the transfected HeLa cells compared to control transfected cells. Using RT-PCR, the effect of two different cathepsin B siRNAs on cathepsin B mRNA expression was investigated. As shown in Fig. 1B, using cathepsin B specific siRNA 1 (cat B-1) only a suppression of cathepsin B mRNA to 40.5 ± 22.5% was seen whereas siRNA 2 (cat B-2) caused a reduction of the target mRNA to 4.3 ± 1.9% compared to control transfectants. Therefore, cells transfected with siRNA 2 were further analyzed for cathepsin B protein and activity. Cathepsin B was almost undetectable through immunoblotting in HeLa cells transfected with siRNA 2 (Fig. 1C) and cathepsin B activity was significantly decreased from 37.5 ± 7.8 μmol/mg × h compared in control transfectants to 1.75 ± 0.32 μmol/mg × h in cells transfected with siRNA 2 (Fig. 1D).

Hence, for all further experiments HeLa cells transfected with cat B-2 siRNA was used for comparison analysis of a role of cathepsin B in doxorubicin-induced cell death.

3.3. Impact of cathepsin B suppression on cathepsin D, cathepsin L and Caspase 1

To investigate whether siRNA-mediated cathepsin B suppression influences the protein expression of other cathepsins being relevant in apoptotic processes we performed immunoblot analyses with cathepsin D and L specific antibodies. As shown in Fig. 1E, neither a co-suppression of cathepsin D or L nor a counterregulation for compensation of cathepsin B deficiency was caused by cathepsin B specific siRNA 2 (cat B-2).

Since it is known that cathepsin B can mediate cleavage of Caspase 1 precursor to an intermediate fragment [20], we determined Caspase 1 protein using immunoblot analysis to

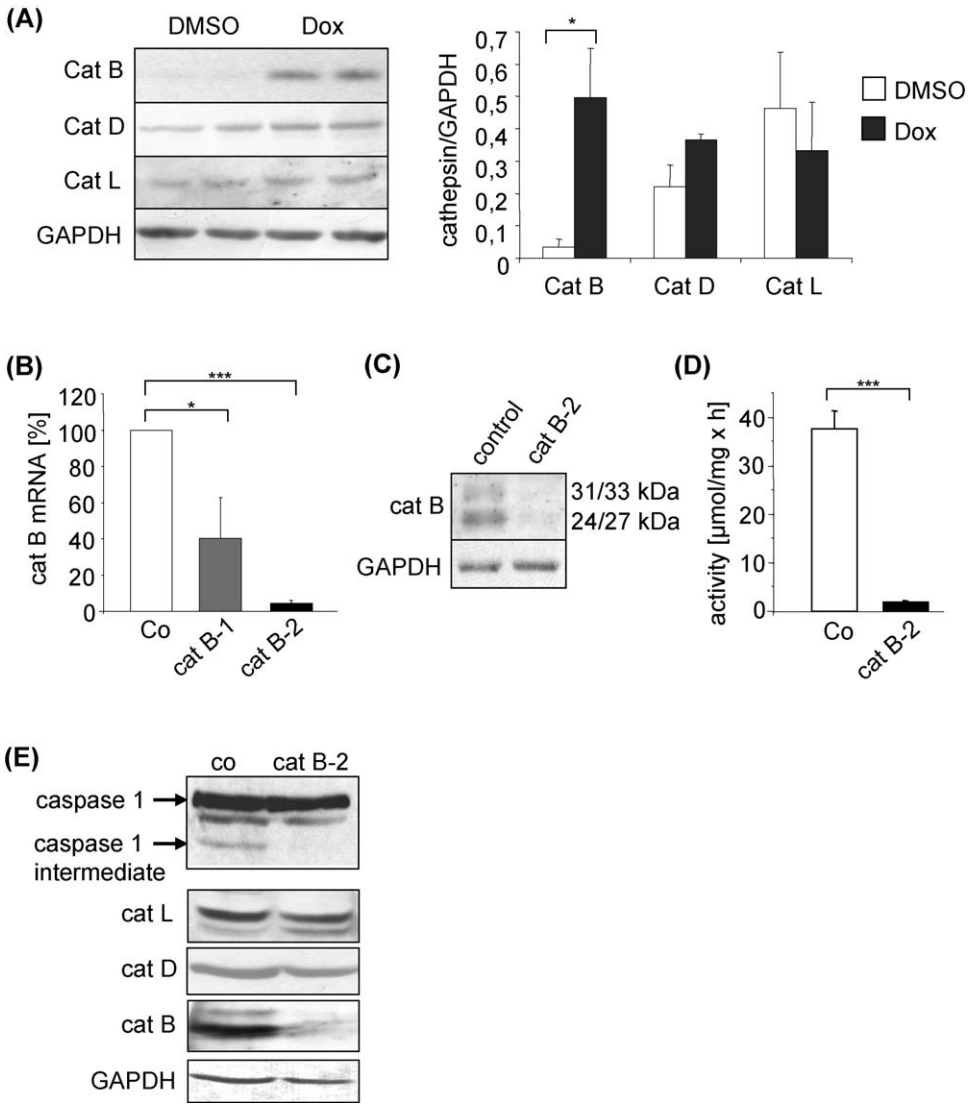

Fig. 1. Regulation of cathepsins. (A, left) Immunoblot analysis of cathepsin B, D and L in control (DMSO) or doxorubicin (1 μM) treated HeLa cells after 48 h. (A, right) Densitometric evaluation of cathepsin protein expression, $n = 3$. (B) Expression of cathepsin B mRNA in control transfectants (Co), cells transfected with siRNA 1 (cat B-1) or with siRNA 2 (cat B-2), $n = 3$, normalization to 18S rRNA. (C) Immunoblot analysis of cathepsin B protein in control transfectants (Co) and cells transfected with siRNA 2 (cat B-2). (D) Cathepsin B activity in control transfected cells (Co) and cells transfected with siRNA 2 (cat B-2) determined by Z-AMC assay, $n = 4$. (D) Expression of cathepsin B, D and L as well as Caspase 1 in control transfectants (co) and cells with siRNA 2 (cat B-2) determined by immunoblotting.

further check the loss of cathepsin B function in the knockdown cells. In control transfected cells, a Caspase 1 signal at 45 kDa and at about 38 kDa were apparent representing the Caspase 1 precursor and the intermediate isoform, respectively. In contrast to this, in cathepsin B suppressed cells only a signal at 45 kDa was seen demonstrating the functional consequences of the cathepsin B knockdown (Fig. 1E).

3.4. Influence of cathepsin B suppression on activation of Caspase 3, 8 and 9 as well as PARP cleavage

Using commercially available substrates, we determined the activity of Caspase 3, 8 and 9 in control transfectants and cathepsin B knockdown cells after 0, 24, 48 and 72 h. Treatment of control and cat B-2 siRNA transfected HeLa cells with doxorubicin results in a time-dependent activation of Caspase 3 with values of 104.1%, 148.9%, 205.2% and 227% in control transfectants and with 111.6%, 112.5%, 125.8% and 174.7% in cathepsin B suppressed cells representing significantly decreased Caspase 3 activation (Fig. 2A-left). In addition, pre-incubation with the cathepsin B inhibitor CA074Me also reduced doxorubicin-induced Caspase 3 activity (Fig. 2A-right). In contrast to Caspase 3, there was no significant difference in Caspase 8 and 9 activity level between control transfectants and cathepsin B suppressed cells (Fig. 2B and C).

Caspase 3 activation confirmed by immunodetection of cleaved PARP in control transfected as well as in cells with transfection of cat B-2 siRNA. As shown in Fig. 2D, the amount of cleaved PARP after 72 h of doxorubicin treatment was significantly lesser in cathepsin B suppressed cells (AU 0.20 ± 0.03) compared with that in control transfectants (AU 0.29 ± 0.04).

3.5. Cathepsin B silencing reduces doxorubicin-mediated loss of mitochondrial membrane potential ($\Delta\Psi m$) and release of mitochondrial proteins

The loss of $\Delta\Psi m$ was monitored using TMRE which decreases its fluorescence upon breakdown of $\Delta\Psi m$. The number of cells with decreased fluorescence increased over the time of doxorubicin treatment in control transfected as well as in cathepsin B

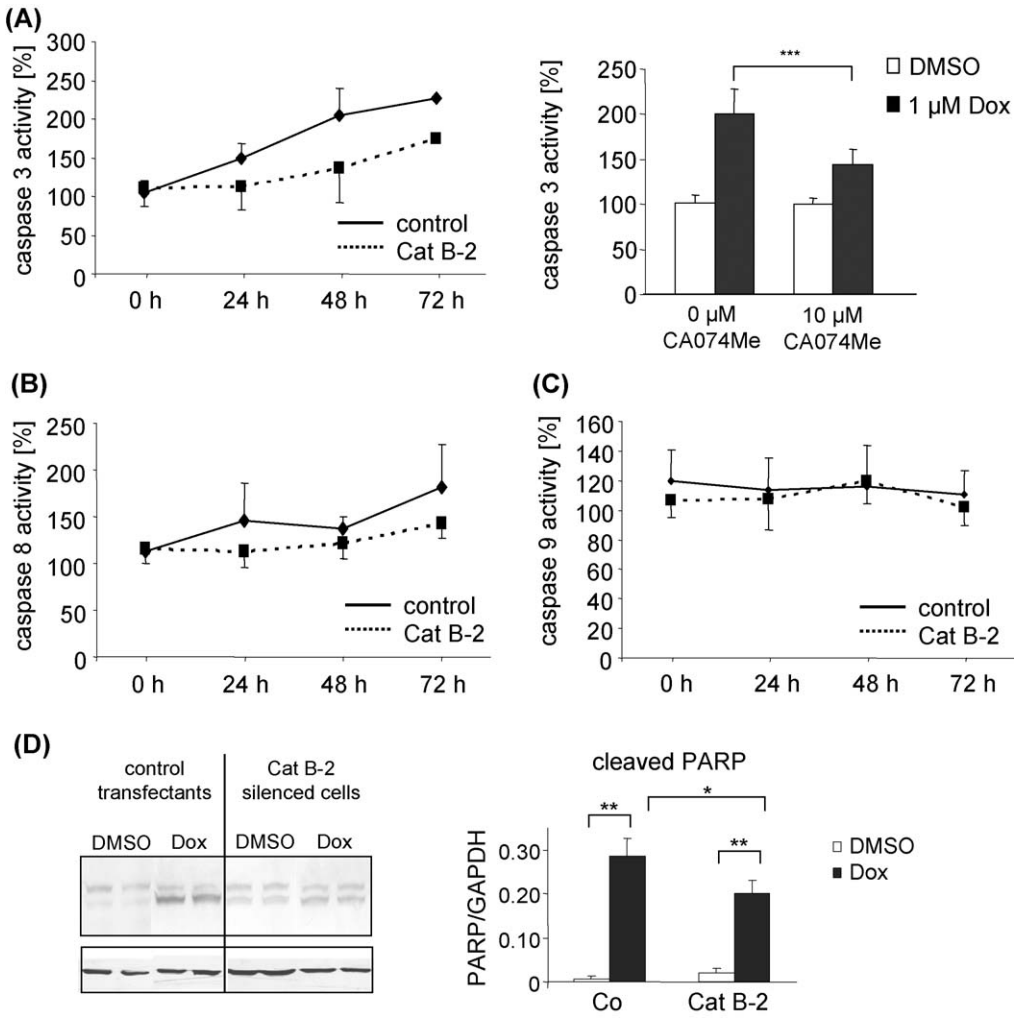

Fig. 2. Influence of cathepsin B suppression on doxorubicin-induced activation of Caspase 3, 8 and 9 as well as PARP cleavage. (A-left) HeLa control transfectants (Co) and cathepsin B suppressed cells (cat B-2) were incubated with DMSO or doxorubicin (1 μM) and after 0, 24, 48 or 72 h the activity of Caspase 3 was determined. (A-right) Doxorubicin-induced Caspase 3 activity with or without pre-treatment with 10 μM of CA074Me, $n = 3$. (B) Caspase 8 and (C) Caspase 9 activity was determined using specific substrates for each caspase. DMSO treated cells were set as 100% and doxorubicin treated cells were related to this. Mean ± SD of three independent experiments each in triplicate. (D-left) Cleavage of PARP in control transfectants and cathepsin B suppressed cells (cat B-2) 72 h after doxorubicin (dox) application determined by immunoblot analysis. (D-right) Densitometric evaluation of cleaved PARP, $n = 3$.

knockdown cells with no significant differences at 24 and 48 h (Fig. 3A). In contrast, at the later time points a difference in loss of mitochondrial integrity was seen with the most significant discrepancy at 72 h after doxorubicin application showing a mitochondrial integrity of 20.8 ± 1.73% in control transfectants (Co) versus 37.7 ± 5.75% in cathepsin B silenced cells (cat B-2). Untreated control transfectants and cathepsin B suppressed cells showed no loss of $\Delta\Psi$m within the first 48 h and only marginal loss of $\Delta\Psi$m at the later time points which was not significantly different between control transfected and cathepsin B silenced cells (not shown). Additionally, we checked the influence of the cathepsin B specific inhibitor CA074Me as well as of the Caspase 3 inhibitor Z-DEVD-fmk on doxorubicin-mediated loss of mitochondrial membrane potential at 64 h of treatment. As demonstrated in Fig. 3B(left + right) both inhibition of cathepsin B by CA074Me (10 μM) and of Caspase 3 by Z-DEVD-fmk (10 μM) resulted in a significantly reduced doxorubicin induced loss $\Delta\Psi$m. In control transfectants, intact mitochondrial membrane potential was increased from 35.9 ± 0.77% upon doxorubicin alone to 75.2 ± 1.36% and 76.3 ± 0.81% by co-treatment with CA074Me and Z-DEVD-fmk, respectively. In cathepsin B suppressed cells, intact mitochondrial membrane potential was also elevated from 57 ± 3.78% upon doxorubicin alone to 70.3 ± 3.13% and 71.1 ± 4.08% by additional application of CA074Me and Z-DEVD-fmk, respectively, but these differences were not so pronounced as in control transfected cells (Fig. 3B).

Having shown a major loss $\Delta\Psi$m upon doxorubicin, we next studied the release of cytochrome C and AIF into cytosol. For both cytochrome C and AIF, in cathepsin B silenced HeLa cells the release was significantly reduced after doxorubicin treatment compared to control transfected cells. As shown in Fig. 3C, cytochrome C release in control transfected cells upon doxorubicin treatment was induced to 1131 ± 117% and 2302 ± 792% compared to the untreated control and in cathepsin B silenced cells to only 345 ± 125% and 569 ± 292% after 48 and 72 h, respectively. AIF release in control transfected cells was enhanced to 507 ± 147% and 2926 ± 646% and in cathepsin B silenced cells only to 242 ± 153% and 259 ± 57% after 48 and 72 h, respectively (Fig. 3D).

3.6. Influence of cathepsin B suppression on regulation of members of the Bcl-2 family, XIAP and p53

Apoptosis is accompanied by up-regulation of the pro-apoptotic Bcl-2 family member Bax, which is involved in the mitochon-

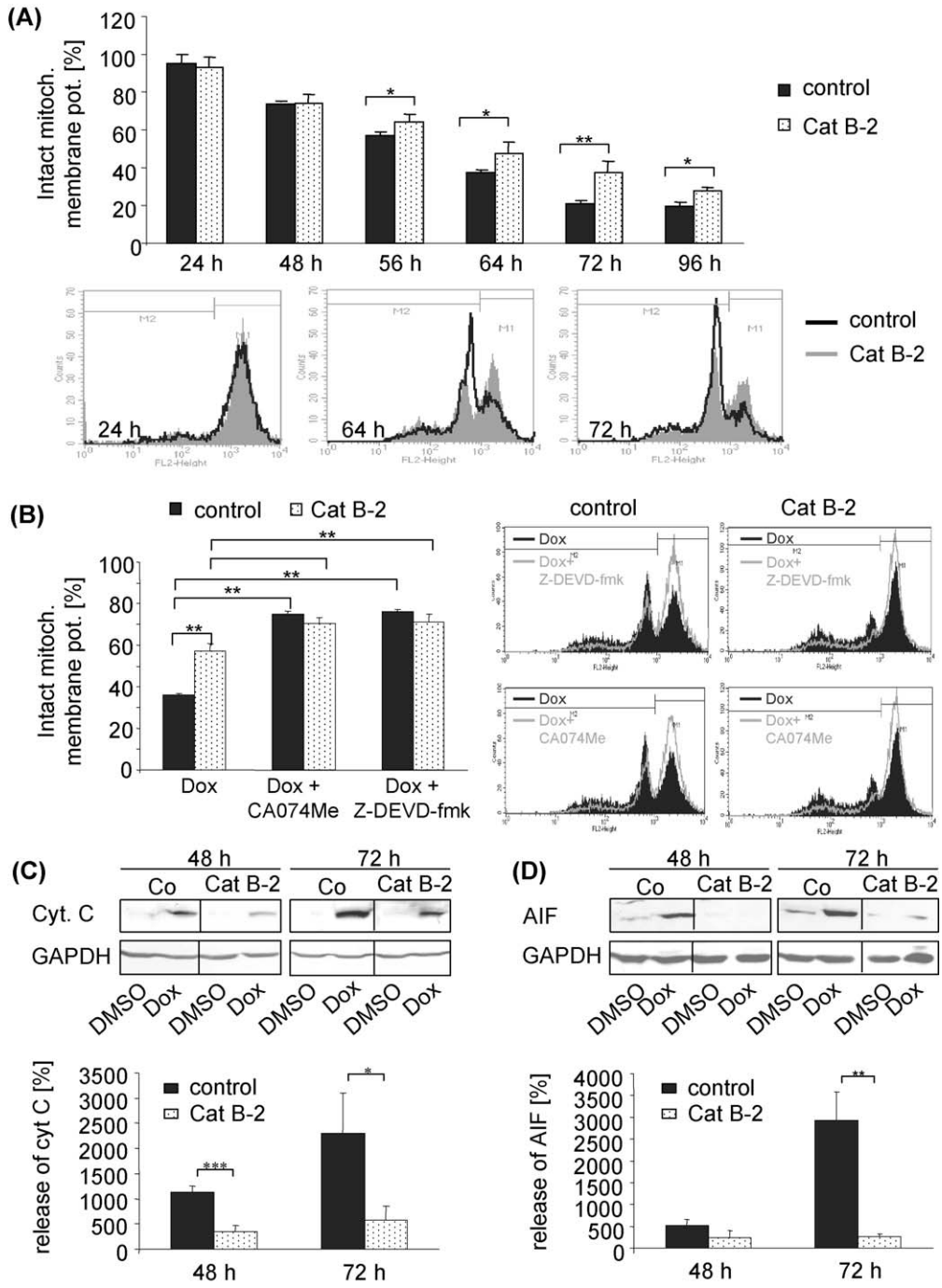

Fig. 3. Influence of cathepsin B silencing on doxorubicin-induced loss $\Delta\Psi$m and release of AIF and cytochrome C into cytosol. (A) Determination of $\Delta\Psi$m with TMRE staining and FACS measurements in doxorubicin treated control transfectants (Co) and cathepsin B silenced cells (cat B-2) at different time points. $n = 4$, mean ± SD. (D) Influence of cathepsin B specific inhibitor CA074Me and Caspase 3 inhibitor Z-DEVD-fmk on doxorubicin induced loss $\Delta\Psi$m in control transfectants (Co) and cathepsin B silenced cells (cat B-2) determined with TMRE staining. Cells were pre-treated for 1.5 h with CA074Me (10 μM) or Z-DEVD-fmk (10 μM) followed by doxorubicin exposure for 64 h. $n = 3$, mean ± SD. (C) Release of cytochrome C into the cytosol detected by immunoblotting, one representative figure of four independent experiments. The respective DMSO control was set as 100%. (D) Release of AIF into the cytosol detected by immunoblotting, one representative figure of four independent experiments. The respective DMSO control was set as 100%.

drial apoptosis pathway and Bcl-2 has been characterized as potent inhibitor of apoptosis and regulation of this anti-apoptotic protein by doxorubicin is known [21]. We therefore analyzed Bax and Bcl-2 expression in doxorubicin treated control transfectants and cathepsin B suppressed cells. As shown in Fig. 4A and B, both in control transfectants as well as in cathepsin B suppressed cells a down-regulation of Bcl-2 was visible at 72 h. Interestingly, cathepsin B knockdown cells showed a stronger band intensity upon DMSO as well as doxorubicin (AU DMSO 0.67 ± 0.30 and Dox 0.38 ± 0.07) compared to control transfected cells (AU DMSO 0.37 ± 0.15 and Dox 0.18 ± 0.04).

In contrast to Bcl-2, protein levels of the anti-apoptotic Bcl-xL were significantly enhanced by doxorubicin treatment in both control transfectants (AU DMSO 0.32 ± 0.14 and Dox 1.21 ± 0.15) as well as in cathepsin B silenced cells at 72 h (AU DMSO 0.27 ± 0.09 and Dox 1.08 ± 0.03) to a similar content (Fig. 4A and B).

The anti-apoptotic action of Bcl-2 and Bcl-xL is inhibited by the Bcl-2 family member Bax. As demonstrated in Fig. 4A and B, we

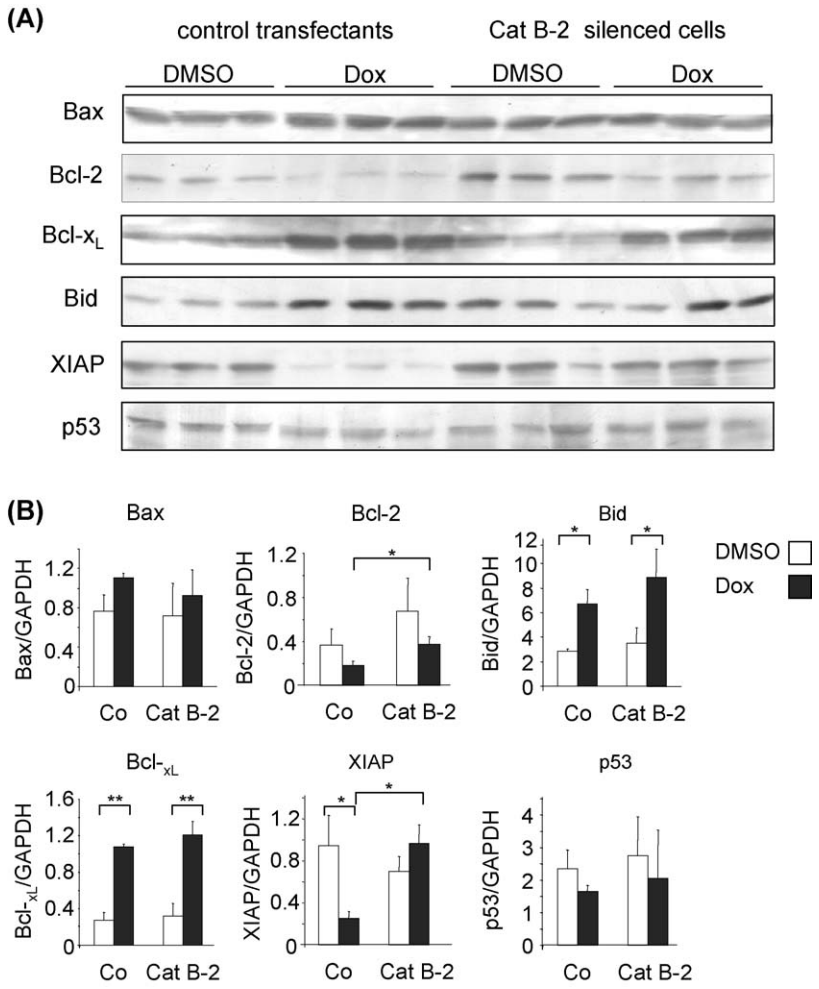

Fig. 4. Influence of cathepsin B suppression on doxorubicin-induced regulation of apoptosis-relevant proteins. HeLa control transfectants (Co) and cathepsin B suppressed cells (cat B-2) were incubated with DMSO (solvent) or doxorubicin (1 μM) for 72 h. (A) The expression of Bax, Bcl-2, Bcl-xL, Bid, XIAP and p53 was analyzed by immunoblot analysis. (B) Densitometric evaluation of three independent experiments with normalization to GAPDH. Mean ± SD, $n = 3$.

found no significant regulation of Bax protein level at 72 h of doxorubicin application in control transfected (AU DMSO 0.76 ± 0.17 and Dox 1.10 ± 0.05) or in cathepsin B silenced cells (AU DMSO 0.72 ± 0.33 and Dox 0.92 ± 0.26).

Another pro-apoptotic molecule involved in mitochondrial apoptosis pathway is Bid which is processed during apoptosis to the active truncated Bid (tBid). We detected neither Bid cleavage nor any disappearance of the full-length Bid in doxorubicin-treated HeLa cells. In contrast, a similar and significant increase in the full-length Bid was seen in both control transfectants (AU DMSO 2.83 ± 0.24 and Dox 6.74 ± 1.16) and cathepsin B knockdown cells (AU DMSO 3.52 ± 1.25 and Dox 8.72 ± 2.12) (Fig. 4A and B).

Since it has been shown that doxorubicin induced p53 expression and can activate p53 dependent apoptosis [22], we characterized expression of p53 in our cell model. As shown in Fig. 4A and B, treatment of HeLa cells with doxorubicin for 72 h did not significantly change p53 protein levels in control transfectants (AU DMSO 2.34 ± 0.58 and Dox 1.66 ± 0.19) and cathepsin B knockdown cells (AU DMSO 2.76 ± 1.19 and Dox 2.05 ± 1.48).

XIAP (X-chromosome linked inhibitor of apoptosis) is described as an anti-apoptotic protein that mediates degradation of Caspase 3 [23]. Since Caspase 3 activation was diminished in cathepsin B silenced cells, we also evaluated protein level of this Caspase 3 inhibiting protein. As demonstrated in Fig. 4A and B, a significant diminished XIAP band was seen only in control transfectants with AU from 0.94 ± 0.29 (DMSO) to 0.25 ± 0.07 (Dox). In contrast, in cathepsin B knockdown cells XIAP was not down-regulated (AU DMSO 0.70 ± 0.14 and Dox 0.96 ± 0.18).

In addition, at 48 h after doxorubicin application no significant alteration in protein expression was seen for Bax, Bid, Bcl-2, Bcl-xL and p53 and a down-regulation for XIAP (data not shown).

3.7. Influence of cathepsin B suppression on cell cycle regulatory proteins

It has been described in detail in various tumor cell models that doxorubicin results in an arrest in the G_2M phase [24]. The underlying modification of cell cycle regulatory proteins, however, has not been addressed in extenso.

Treatment of both control and cathepsin B suppressed cells resulted in significantly enhanced expression, phosphorylation and therefore inactivation of the kinase cdk1. Interestingly, whereas the induction of cdk1 protein expression upon doxorubicin at 72 h was similar in control transfected (AU DMSO 0.17 ± 0.09 and Dox 0.67 ± 0.08) and cathepsin B silenced cells (AU DMSO 0.10 ± 0.03 and Dox 0.61 ± 0.21), the phosphorylation was significantly stronger in cathepsin B knockdown cells (AU DMSO 0.18 ± 0.02 and Dox 1.35 ± 0.30) compared to the parental cells (AU DMSO 0.29 ± 0.09 and Dox 0.68 ± .12) (Fig. 5A and B).

Since Wee1 and Myt1 are known to be responsible for phosphorylation of cdk1 [25], we next investigated expression and phosphorylation of these two kinases. As shown in Fig. 5A and

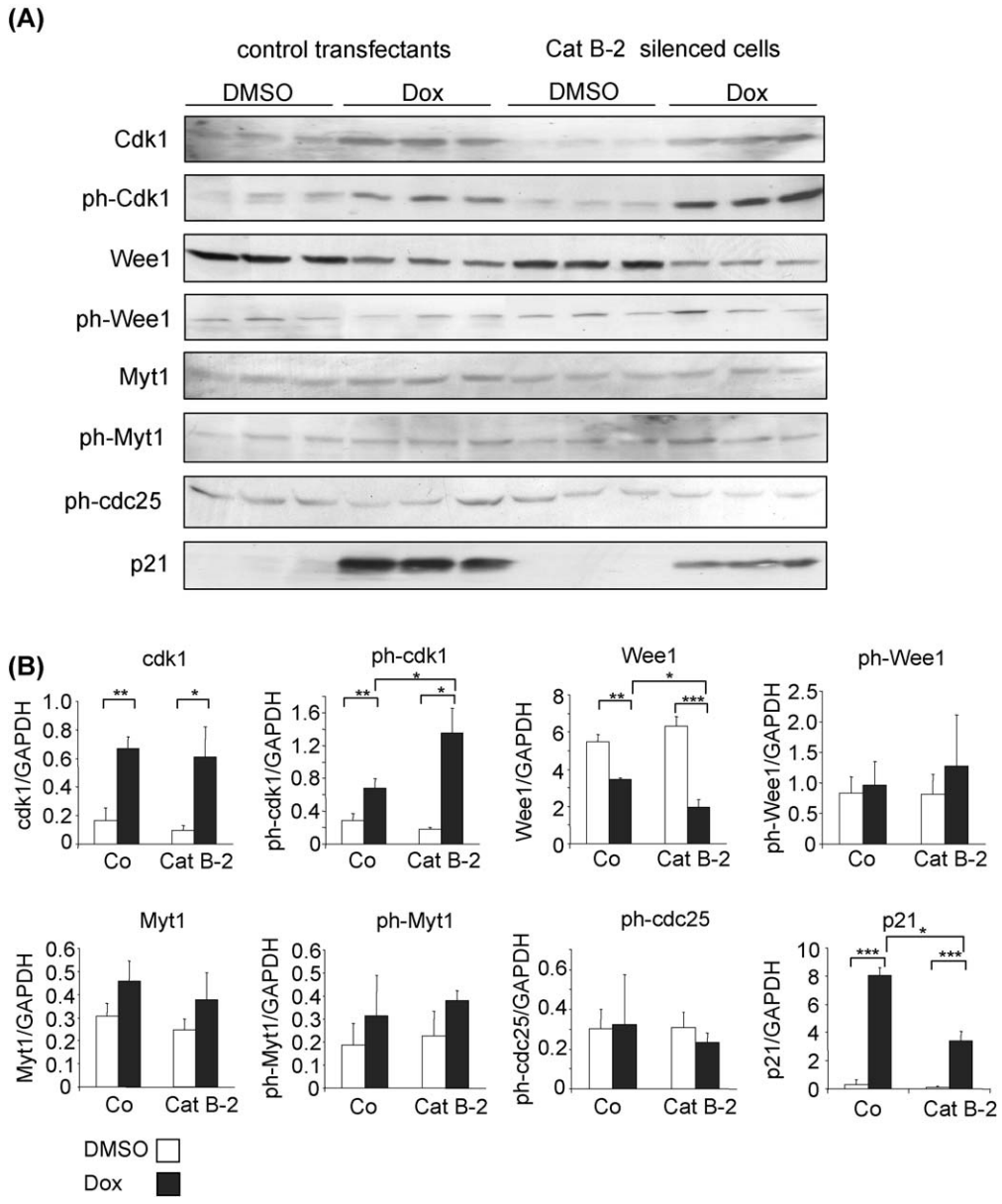

Fig. 5. Influence of cathepsin B suppression on cell cycle regulatory proteins. HeLa control transfectants and cathepsin B silenced cells (cat B-2) were incubated with DMSO (solvent) or doxorubicin (1 μM) for 72 h. (A) The expression of total and phosphorylated forms of cdk1, Wee1, Myt1 and cdc25 as well as p21 was analyzed by immunoblot analysis. (B) Densitometric evaluation of three independent experiments with normalization to GAPDH. Mean ± SD, $n = 3$.

B, protein content and phosphorylation of Myt1 was slightly but not significantly changed upon doxorubicin at 72 h in control transfectants and cathepsin B suppressed cells. For Wee1, a significant reduction in protein expression was observed 72 h after doxorubicin application in control transfectants (AU DMSO 5.50 ± 0.37 and Dox 3.46 ± 0.08) and cathepsin B suppressed cells (AU DMSO 6.28 ± 0.56 and Dox 1.92 ± 0.47). Interestingly, there was no concomitant decrease in the phosphorylation status of Wee1 in both control transfected (AU DMSO 0.84 ± 0.26 and Dox 0.96 ± 0.39) and cathepsin B silenced cells (AU DMSO 0.81 ± 0.32 and Dox 1.27 ± 0.84) (Fig. 5A and B).

Another cdk1 regulator is the phosphatase cdc25 responsible for activation of cdk1 through its dephosphorylating activity [25]. As demonstrated in Fig. 5A and B, doxorubicin application for 72 h caused no change in the phosphorylated forms of cdc25 on cells transfected with the control vector (AU DMSO 0.30 ± 0.10 and Dox 0.32 ± .025) as well as in cells with cathepsin B knockdown (AU DMSO 0.31 ± 0.08 and Dox 0.23 ± 0.05).

During the cell cycle, cdk1 is regulated in part by the cyclin-dependent kinase inhibitor p21 [26]. In our HeLa cell model, doxorubicin treatment caused a strong induction of p21 expression which was significantly reduced in cathepsin B silenced cells (AU DMSO 0.11 ± 0.08 and Dox 3.34 ± 0.62) compared to cells transfected with the control vector (AU DMSO 0.31 ± 0.34 and Dox 8.06 ± 0.53) (Fig. 5A and B).

Notable, at 48 h no significant regulation upon doxorubicin was seen for cdk1, Myt1, phosphorylated Myt1, phosphorylated Wee1 and phosphorylated cdc25 whereas phosphorylated cdk1 and p21 were also increased (data not shown).

3.8. Influence of cathepsin B suppression on cell cycle phases and overall cell viability

Since as described above doxorubicin treatment caused changes in some of the investigated cell cycle regulatory proteins, we next investigated whether this translates in alteration

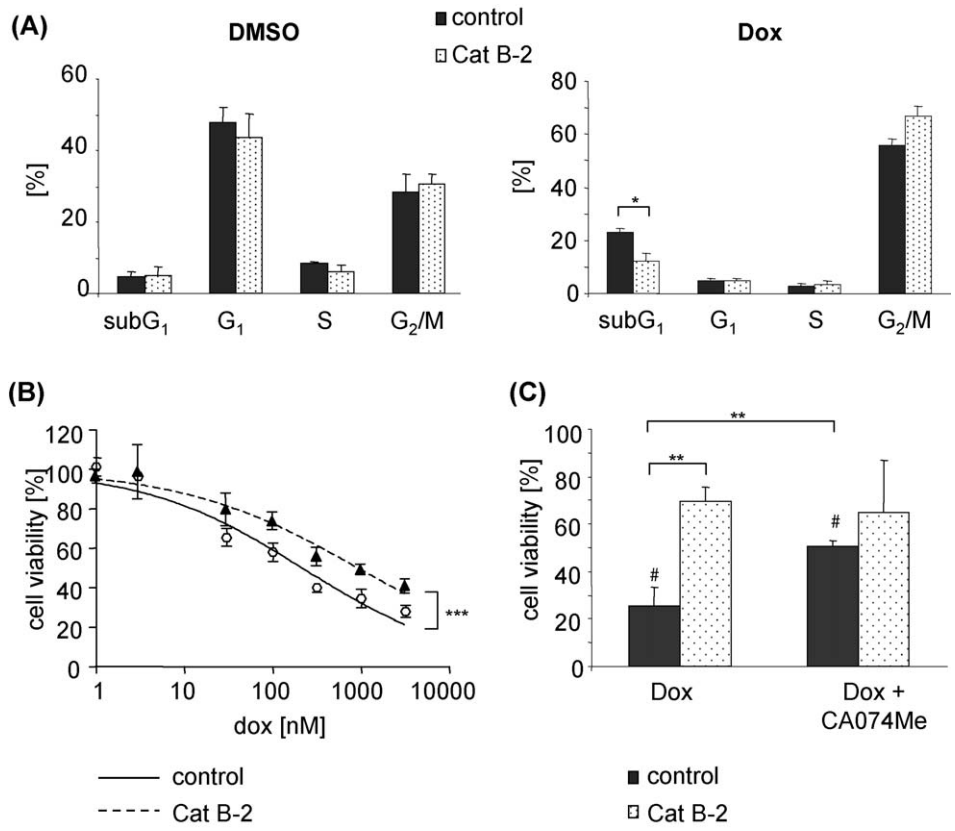

Fig. 6. Influence of cathepsin B suppression on cell cycle phases and overall cell viability (A) Cell cycle analysis using propidium iodide staining of DNA content by FACS analysis. HeLa control transfectants (Co) and cathepsin B silenced cells (cat B-2) were incubated with DMSO or doxorubicin (1 μM) for 72 h followed by incubation with propidium iodide FACS analysis. Mean ± SD, $n = 5$. (B) HeLa control transfectants (Co) and cathepsin B silenced cells (cat B-2) were incubated with DMSO or doxorubicin for 72 h followed by determination of cell viability using Alamar Blue™ Staining. Mean ± SD, $n = 3$. (C) Pre-treatment of Hela control transfected and cathepsin B knockdown cells with cathepsin B inhibitor CA074Me (10 μM) for 1.5 h followed by application of doxorubicin (1 μM) for 70 h and analyzed using Alamar Blue™ Staining. Mean ± SD, $n = 3$. DMSO treated cells were set as 100%. The # represents significant differences to the DMSO control ($p < 0.005$).

regarding cell cycle phases. As shown in Fig. 6A no significant changes in subG$_1$, G$_1$, S and G$_2$M cell cycle phases were seen upon treatment with the solvent DMSO in control transfectants versus cathepsin B silenced cells after 72 h of treatment. Interestingly, despite different regulations of some cell cycle regulatory proteins (p21, phosphorylated cdk1) 72 h after doxorubicin application a significant increase in G$_2$/M phase was induced in both control transfectants as well as in cathepsin B silenced cells. This rise in the G$_2$/M fraction was slightly but not significantly more pronounced in cathepsin B knockdown cells (67 ± 3.2%) than in control transfectants (55.7 ± 2.3%). In contrast, doxorubicin induced increase in subG$_1$ fraction was significantly reduced about half in cathepsin B silenced cells (12.5 ± 2.7%) compared with control transfected cells (23.1 ± 1.5%) (Fig. 6A-right).

The Alamar Blue assay was used to evaluate the influence of cathepsin B suppression on overall cell viability after doxorubicin application and to determine the IC$_{50}$ in control transfected HeLa cells and cathepsin B silenced cells. As shown in Fig. 6B, suppression of cathepsin B partially restored cell viability. The IC$_{50}$ values obtained after 72 h by Alamar Blue assay were significantly different between control transfectants (214.4 nM) and cathepsin B knockdown cells (946.7 nM). Furthermore, pre-treatment of control transfected cells with cathepsin B specific inhibitor CA074Me (10 μM) followed by application of 1 μM doxorubicin for 72 h significantly enhanced cell viability from 25 ± 7.8% (doxorubicin alone) to 51 ± 2.4% (doxorubicin + CA074Me) whereas in cathepsin B suppressed cells no additional effects of CA074Me were observed (70 ± 5.8% for doxorubicin alone and 65 ± 22.2% for doxorubicin + CA074Me, Fig. 6C).

3.9. Impact of cathepsin B expression on cytotoxicity of doxorubicin in different tumor cell lines

To test whether cathepsin B expression is important for cytotoxic response to doxorubicin in other tumor cells, we determined the IC$_{50}$ values for doxorubicin in a panel of tumor cell lines (Caco2, colon carcinoma; HeLa, parental cervix carcinoma cells used for cathepsin B silencing experiments; HepG2, hepatocellular carcinoma; PaTuO2, pancreatic adenocarcinoma; LN18, glioblastoma multiforme; U87-MG, astrocytoma) and correlated these with intracellular cathepsin B protein expression. As seen in Fig. 7, the investigated cell lines all express cathepsin B protein but at different levels. While Caco2 cells have the lowest cathepsin B expression level and were rather insensitive to doxorubicin with a calculated IC$_{50}$ value of about 2 mM, the astrocytoma cell line U87-MG showed the highest cathepsin B protein expression and the IC$_{50}$ value was only 96 nM. Correlation analysis using Spearman's nonparametric correlation yielded a negative correlation (Spearman r: −0,8857; $p = 0.033$) between cathepsin B expression and efficacy of doxorubicin which suggests that cathepsin B is involved in doxorubicin toxicity in a range of cell lines and that its loss might account for inherent doxorubicin resistance.

3.10. Expression of cathepsin B in doxorubicin sensitive and resistant cells

Doxorubicin sensitive cell lines can be transformed into resistant cells by treatment with continuously increasing doxorubicin concentrations over a period of several months. To further check

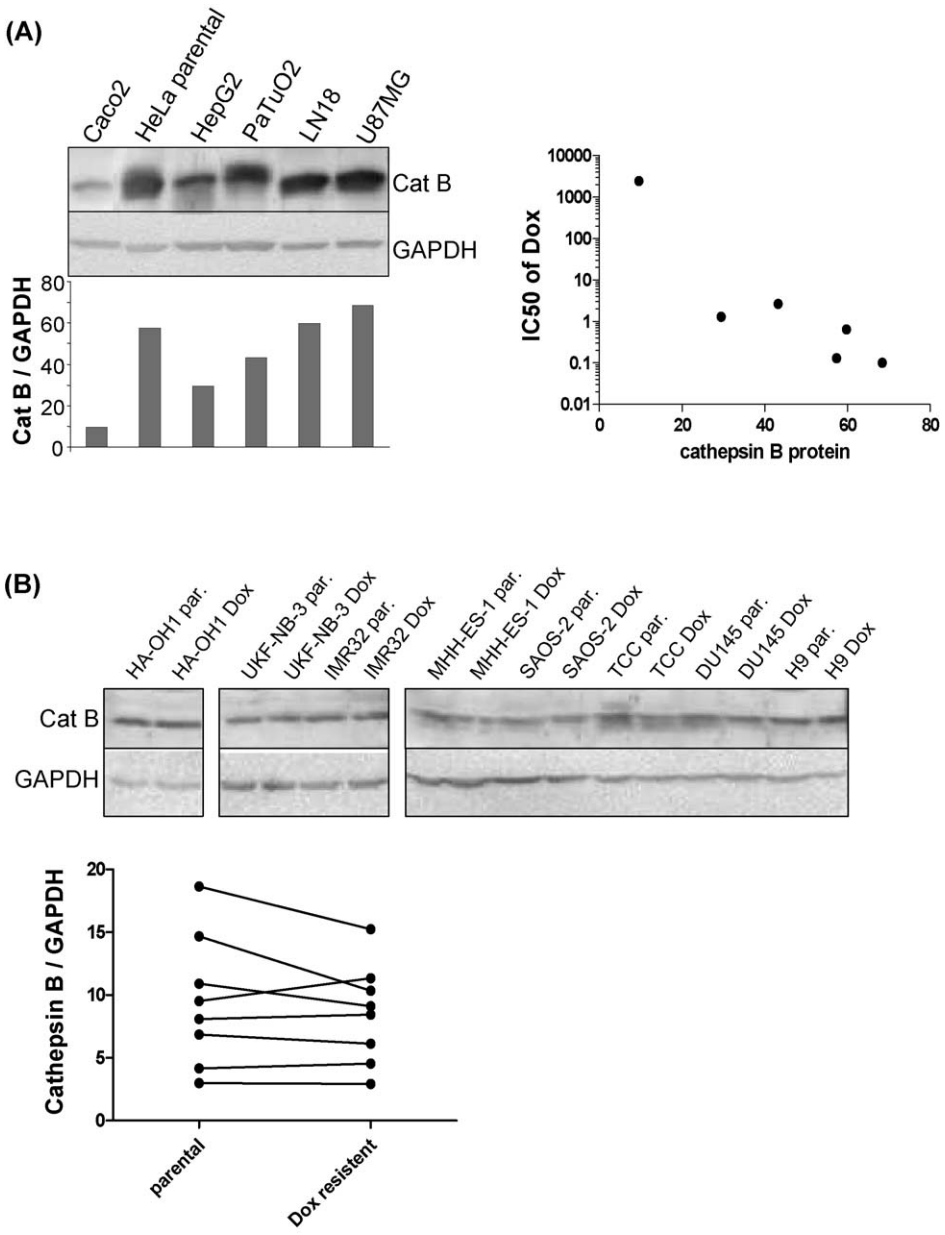

Fig. 7. Influence of cathepsin B protein expression on susceptibility towards doxorubicin in different cell lines. (A) Detection of cathepsin B protein by immunoblot analysis in tumor cell lines of different tumor entities and its correlation to the IC_{50} values of doxorubicin determined using Alamar Blue staining. Correlation of IC_{50} values with cathepsin B protein expression was analyzed by Spearman's nonparametric correlation. (B) Expression of cathepsin B protein in a panel of parental doxorubicin-sensitive (par.) versus doxorubicin-resistant (Dox) cell lines of different origin determined by immunoblot analysis. Doxorubicin-resistant cells were established by continuous adaptation towards doxorubicin.

whether a reduced cathepsin B expression is the reason for this acquired doxorubicin resistance we analyzed the cathepsin protein level in eight pairs of doxorubicin sensitive (parental) and resistant cell lines. As shown in Fig. 7B, Western blot analysis demonstrated that all cells express cathepsin B. Comparison of doxorubicin sensitive with resistant cells revealed that cathepsin B expression was very similar or only slightly reduced in the resistant cell types. Statistical analysis using paired *t*-tests revealed no significant differences. This implies that acquired resistance to doxorubicin seems not to be based on a reduced cathepsin B expression.

4. Discussion

Despite its widespread clinical use the mechanism underlying doxorubicin-triggered apoptosis is not completely characterized. Extrinsic, death receptor mediated as well as intrinsic, mitochondria controlled apoptosis contribute to doxorubicin's mode of action [27,28]. Activation of caspases seems not to be mandatory for cell death upon doxorubicin [16–18] suggesting the presence of additional factors. In the last decade numerous reports highlight the potential role of cathepsin B in controlling apoptosis but its role in drug induced apoptosis has not been addressed in a systematic manner. Using non-specific pharmacological inhibitors evidence pointed to an involvement in cell death induced by bortezomib, paclitaxel and camptothecin [8,9]. Previous experiments indicated selective up-regulation of cathepsin B by doxorubicin but not by other anticancer drugs tested [11]. Expression of apoptosis-relevant cathepsin D and L are not affected by doxorubicin suggesting that cathepsin B maybe the major player in our model. Since pharmacological cathepsin B inhibitors are considered to

block also other proteases [29] a specific knockdown of cathepsin B seems to be a favourable approach for studying the role of this protease in drug induced cell death. Using RNA interference with stable retroviral infection of specific cathepsin B siRNA we demonstrate significant contribution of cathepsin B in doxorubicin-induced cell death.

We first analyzed the impact of cathepsin B silencing on activation of Caspase 3 following doxorubicin. Although Caspase 3 was shown to be a poor substrate of cathepsin B *in vitro*, several studies have shown that inhibition of cathepsin B results in a reduced Caspase 3 activation [3,4] which is in agreement with our results that cathepsin B silencing and inhibition by CA074Me [30] resulted in a significantly reduced Caspase 3 activation and diminished cleavage fragments of PARP in the cathepsin B knockdown cells.

The expression of XIAP (X-chromosome linked inhibitor of apoptosis), an anti-apoptotic protein that mediates degradation of Caspase 3 [23], was reduced in control transfected but not in cathepsin B suppressed cells. This suggests a possible involvement of cathepsin B in XIAP degradation, as suggested by Droga-Mazovec [31], and is in accordance with the diminished Caspase 3 activity in cathepsin B suppressed cells.

Growing evidence supports the participation of mitochondrial dysfunction in cathepsin B-mediated apoptosis [10,32]. In our model, cathepsin B suppressed cells showed a significantly lesser decline of intact mitochondrial membrane potential after 56–96 h of doxorubicin application. Therefore, the preventing effect of cathepsin B knockdown on loss of mitochondrial membrane potential is apparent after up-regulation of cathepsin B [11]. Interestingly, treatment with the Caspase 3 inhibitor Z-DEVD-fmk also resulted in reduced loss of mitochondrial permeability suggesting that Caspase 3 signals a mitochondrial amplification loop as shown in Granzyme B-mediated apoptosis [33].

It was found that cathepsin B attacks mitochondria through processing of Bid [34]. Bid cleavage, however, could not be detected following doxorubicin whereas the full-length form of Bid was strongly present in untreated and doxorubicin-treated control transfected as well as in cathepsin B suppressed cells. These data suggest a minor role of Bid cleavage in doxorubicin-induced apoptosis in our model confirming that cathepsins are still able to promote apoptosis even in the absence of Bid processing [35].

Mitochondrial permeabilization causes release of AIF and cytochrome C from mitochondrial interspace to the cytosol [16]. In TNFα-treated hepatocytes cathepsin B enhances mitochondrial release of cytochrome C [32] and cathepsin B silencing in HeLa cells blocks granulysin-mediated release of cytochrome C and AIF [36]. For both cytochrome C and AIF a strongly reduced release into cytosol was seen in our cathepsin B silenced cells. For AIF a caspase-independent translocation from mitochondria to the nucleus inducing nuclear apoptosis through chromatin condensation and DNA fragmentation was demonstrated [37]. Both chromatin condensation and DNA fragmentation are known to be a consequence of doxorubicin treatment in tumor cells [38] suggesting that AIF could be a potential mediator of these processes. Furthermore, in several models AIF can trigger the release of cytochrome C from mitochondria [39] and could therefore compensate the missing function of truncated Bid in our model.

Permeabilization of the outer membrane of mitochondria is regulated by proteins of the Bcl-2 family [40]. Bcl-2 and Bcl-xL inhibit apoptosis by preventing mitochondria membrane permeabilization. Doxorubicin-induced apoptosis both in control transfectants as well as in cathepsin B silenced cells translated in a down-regulation of Bcl-2 upon doxorubicin. In contrast to Bcl-2, Bcl-xL was significantly increased upon doxorubicin in both control transfectants as well as cathepsin B suppressed cells which could act as compensatory factor for Bcl-2 down-regulation.

To clarify whether suppression of cathepsin B has any impact on the cell cycle, we investigated whether a differential modulation of cell cycle regulators upon doxorubicin occurred. Phosphorylation and thereby inactivation of cdk1 (cyclin dependent kinase 1) was significantly stronger in cathepsin B knockdown cells. Cdk1 inactivation has been reported to decrease the fraction of cells entering apoptosis [41] which is in agreement with our finding of a reduced subG$_1$ fraction in the cathepsin B silenced cells.

Phosphorylation of cdk1 is carried out by Wee1 and Myt1 kinases which are also inhibited by phosphorylation [25]. Additionally, the inhibitory phosphorylation of cdk1 is removed by the cdc25 protein phosphatase [25] but upon doxorubicin activity of cdc25 was not changed. Concerning Myt1 and Wee1 phosphorylation, there was an unchanged level of active protein. Thus, doxorubicin leads to inhibition of cdk1 through phosphorylation but this seems not to be influenced by Wee1, Myt1 or cdc25.

During the cell cycle, cdk1 is regulated in part by the cyclin-dependent kinase inhibitor p21 [26]. Expression of p21, which negatively regulates cdk activity and mediates growth arrest in the G$_2$ phase [42], was up-regulated without induction of p53 expression as already shown [43]. Interestingly, at 72 h the doxorubicin-mediated increase of p21 was significantly stronger in control transfectants than in cathepsin B knockdown cells. An elevated protein level of p21 upon doxorubicin was already shown for senescent cells [44] but preliminary experiments in our HeLa model by using a clonogenic assay showed that both control transfected as well as cathepsin B silenced cells lost the ability to form colonies in a similar matter at a doxorubicin concentration of 1 μM precluding cathepsin B as important determinant in senescence and clonogenicity in our cell model. The senescent phenotype distinguishes cells that survived drug exposure but lost their capacity to divide from those that recover and proliferate further.

Based on the results above we investigated whether changes in cell cycle regulatory proteins, have functional consequences on the cell cycle. Doxorubicin induced increase in subG$_1$ fraction was significantly reduced to about 50% in cathepsin B silenced cells. Of note, the observed increase in G$_2$/M phase was not significantly different between control transfectants and cathepsin B silenced cells suggesting further function of p21 and cdk1 in cell death beside its role in cell cycle control.

Finally, we performed the Alamar Blue assay to evaluate the influence of cathepsin B suppression on overall cell viability after doxorubicin treatment. 72 h after doxorubicin application IC$_{50}$ values were 4.4-fold higher in cathepsin B silenced compared with control transfected cells and CA074Me pre-treatment of control cells also enhanced cell viability compared to doxorubicin application alone. In contrast to the almost complete resistance of hepatocytes from cathepsin B −/− mice against TNFα, we could only partially block doxorubicin-induced cell death by silencing of cathepsin B. These results imply that beside cathepsin B-mediated cell death other pathways may be involved in doxorubicin-induced cytotoxicity which has to be analyzed in further studies. Interestingly, cathepsin B expression in different tumor cell lines was correlated with response to doxorubicin as determined in cell viability assays underlining the modulation of doxorubicin cell death through regulation of cathepsin B expression. In contrast, loss of cathepsin B seems not to be a reason for acquired doxorubicin resistance as demonstrated by comparison of a panel of parental doxorubicin sensitive versus the respective resistant cell lines.

In summary, this study demonstrates that cathepsin B-mediated doxorubicin effects are associated with loss of mitochondrial membrane potential, release of cytochrome C and AIF, XIAP reduction, Caspase 3 activation and PARP cleavage, inhibition of cdk1 as well as regulation of p21 indicating a role cathepsin B in

doxorubicin-mediated cell death. Thus, the elevated cathepsin B expression in many tumors [7] carries the potential to modify the action of doxorubicin.

Acknowledgement

This research was supported by a grant of the Wilhelm Sander Foundation to S.B. (Grant no. 2007.105.1).

References

[1] Houseweart MK, Vilaythong A, Yin XM, Turk B, Noebels JL, Myers RM. Apoptosis caused by cathepsins does not require Bid signaling in an in vivo model of progressive myoclonus epilepsy (EPM1). Cell Death Differ 2003;10:1329–35.
[2] Roberts LR, Kurosawa H, Bronk SF, Fesmier PJ, Agellon LB, Leung WY, et al. Cathepsin B contributes to bile salt-induced apoptosis of rat hepatocytes. Gastroenterology 1997;113:1714–26.
[3] Guicciardi ME, Miyoshi H, Bronk SF, Gores GJ. Cathepsin B knockout mice are resistant to tumor necrosis factor-alpha-mediated hepatocyte apoptosis and liver injury: implications for therapeutic applications. Am J Pathol 2001;159:2045–54.
[4] Nagaraj NS, Vigneswaran N, Zacharias W. Cathepsin B mediates TRAIL-induced apoptosis in oral cancer cells. J Cancer Res Clin Oncol 2006;132:171–83.
[5] Mathiasen IS, Hansen CM, Foghsgaard L, Jaattela M. Sensitization to TNF-induced apoptosis by 1,25-dihydroxy vitamin D(3) involves up-regulation of the TNF receptor 1 and cathepsin B. Int J Cancer 2001;93:224–31.
[6] Canbay A, Guicciardi ME, Higuchi H, Feldstein A, Bronk SF, Rydzewski R, et al. Cathepsin B inactivation attenuates hepatic injury and fibrosis during cholestasis. J Clin Invest 2003;112:152–9.
[7] Yan S, Sloane BF. Molecular regulation of human cathepsin B: implication in pathologies. Biol Chem 2003;384:845–54.
[8] Yeung BH, Huang DC, Sinicrope FA. PS-341 (bortezomib) induces lysosomal cathepsin B release and a caspase-2-dependent mitochondrial permeabilization and apoptosis in human pancreatic cancer cells. J Biol Chem 2006;281:11923–32.
[9] Broker LE, Huisman C, Span SW, Rodriguez JA, Kruyt FA, Giaccone G. Cathepsin B mediates caspase-independent cell death induced by microtubule stabilizing agents in non-small cell lung cancer cells. Cancer Res 2004;64:27–30.
[10] Paquet C, Sane AT, Beauchemin M, Bertrand R. Caspase- and mitochondrial dysfunction-dependent mechanisms of lysosomal leakage and cathepsin B activation in DNA damage-induced apoptosis. Leukemia 2005;19:784–91.
[11] Bien S, Ritter CA, Gratz M, Sperker B, Sonnemann J, Beck JF, et al. Nuclear factor-kappa B mediates up-regulation of cathepsin B by doxorubicin in tumor cells. Mol Pharmacol 2004;65:1092–102.
[12] Long III HJ, Rayson S, Podratz KC, Abu-Ghazaleh S, Suman V, Hartmann LC, et al. Long-term survival of patients with advanced/recurrent carcinoma of cervix and vagina after neoadjuvant treatment with methotrexate, vinblastine, doxorubicin, and cisplatin with or without the addition of molgramostim, and review of the literature. Am J Clin Oncol 2002;25:547–51.
[13] Ferrandina G, Lorusso D, Longo R, Testa AC, Scambia G. Pegylated liposomal doxorubicin in platinum-treated recurrent or metastatic cervical carcinoma. Gynecol Oncol 2005;98:332–3.
[14] Minotti G, Menna P, Salvatorelli E, Cairo G, Gianni L. Anthracyclines: molecular advances and pharmacologic developments in antitumor activity and cardiotoxicity. Pharmacol Rev 2004;56:185–229.
[15] Muller I, Niethammer D, Bruchelt G. Anthracycline-derived chemotherapeutics in apoptosis and free radical cytotoxicity (review). Int J Mol Med 1998;1:491–4.
[16] Carter BZ, Kornblau SM, Tsao T, Wang RY, Schober WD, Milella M, et al. Caspase-independent cell death in AML: caspase inhibition in vitro with pan-caspase inhibitors or in vivo by XIAP or Survivin does not affect cell survival or prognosis. Blood 2003;102:4179–86.
[17] Rebbaa A, Zheng X, Chou PM, Mirkin BL. Caspase inhibition switches doxorubicin-induced apoptosis to senescence. Oncogene 2003;22:2805–11.
[18] Hopkins-Donaldson S, Yan P, Bourloud KB, Muhlethaler A, Bodmer JL, Gross N. Doxorubicin-induced death in neuroblastoma does not involve death receptors in S-type cells and is caspase-independent in N-type cells. Oncogene 2002;21:6132–7.
[19] Kotchetkov R, Driever PH, Cinatl J, Michaelis M, Karaskova J, Blaheta R, et al. Increased malignant behavior in neuroblastoma cells with acquired multi-drug resistance does not depend on P-gp expression. Int J Oncol 2005;27:1029–37.
[20] Vancompernolle K, Van Herreweghe F, Pynaert G, Van de CM, De Vos K, Totty N, et al. Atractyloside-induced release of cathepsin B, a protease with caspase-processing activity. FEBS Lett 1998;438:150–8.
[21] Rabizadeh E, Bairey O, Aviram A, Ben Dror I, Shaklai M, Zimra Y. Doxorubicin and a butyric acid derivative effectively reduce levels of BCL-2 protein in the cells of chronic lymphocytic leukemia patient. Eur J Haematol 2001;66:263–71.
[22] Brantley-Finley C, Lyle CS, Du L, Goodwin ME, Hall T, Szwedo D, et al. The JNK, ERK and p53 pathways play distinct roles in apoptosis mediated by the antitumor agents vinblastine, doxorubicin, and etoposide. Biochem Pharmacol 2003;66:459–69.
[23] Riedl SJ, Renatus M, Schwarzenbacher R, Zhou Q, Sun C, Fesik SW, et al. Structural basis for the inhibition of caspase-3 by XIAP. Cell 2001;104:791–800.
[24] Karlseder J, Wissing D, Holzer G, Orel L, Sliutz G, Auer H, et al. HSP70 overexpression mediates the escape of a doxorubicin-induced G2 cell cycle arrest. Biochem Biophys Res Commun 1996;220:153–9.
[25] Morgan DO. Principles of CDK regulation. Nature 1995;374:131–4.
[26] Coqueret O. New roles for p21 and p27 cell-cycle inhibitors: a function for each cell compartment? Trends Cell Biol 2003;13:65–70.
[27] Huigsloot M, Tijdens IB, Mulder GJ, van de WB. Differential regulation of doxorubicin-induced mitochondrial dysfunction and apoptosis by Bcl-2 in mammary adenocarcinoma (MTLn3) cells. J Biol Chem 2002;277:35869–7.
[28] Muller M, Strand S, Hug H, Heinemann EM, Walczak H, Hofmann WJ, et al. Drug-induced apoptosis in hepatoma cells is mediated by the CD95 (APO-1/Fas) receptor/ligand system and involves activation of wild-type p53. J Clin Invest 1997;99:403–13.
[29] Montaser M, Lalmanach G, Mach L. CA-074, but not its methyl ester CA-074Me, is a selective inhibitor of cathepsin B within living cells. Biol Chem 2002;383:1305–8.
[30] Linebaugh BE, Sameni M, Day NA, Sloane BF, Keppler D. Exocytosis of active cathepsin B enzyme activity at pH 7.0, inhibition and molecular mass. Eur J Biochem 1999;264:100–9.
[31] Droga-Mazovec G, Bojic L, Petelin A, Ivanova S, Romih R, Repnik U, et al. Cysteine cathepsins trigger caspase-dependent cell death through cleavage of bid and antiapoptotic Bcl-2 homologues. J Biol Chem 2008;283:19140–5.
[32] Guicciardi ME, Deussing J, Miyoshi H, Bronk SF, Svingen PA, Peters C, et al. Cathepsin B contributes to TNF-alpha-mediated hepatocyte apoptosis by promoting mitochondrial release of cytochrome c. J Clin Invest 2000;106:1127–37.
[33] Metkar SS, Wang B, Ebbs ML, Kim JH, Lee YJ, Raja SM, et al. Granzyme B activates procaspase-3 which signals a mitochondrial amplification loop for maximal apoptosis. J Cell Biol 2003;160:875–85.
[34] Guicciardi ME, Leist M, Gores GJ. Lysosomes in cell death. Oncogene 2004;23:2881–90.
[35] Boya P, Gonzalez-Polo RA, Poncet D, Andreau K, Vieira HL, Roumier T, et al. Mitochondrial membrane permeabilization is a critical step of lysosome-initiated apoptosis induced by hydroxychloroquine. Oncogene 2003;22:3927–3936.
[36] Zhang H, Zhong C, Shi L, Guo Y, Fan Z. Granulysin induces cathepsin B release from lysosomes of target tumor cells to attack mitochondria through processing of bid leading to Necroptosis. J Immunol 2009;182:6993–7000.
[37] Cande C, Cohen I, Daugas E, Ravagnan L, Larochette N, Zamzami N, et al. Apoptosis-inducing factor (AIF): a novel caspase-independent death effector released from mitochondria. Biochimie 2002;84:215–22.
[38] da Silva CP, de Oliveira CR, da Conceicao M, de Lima P. Apoptosis as a mechanism of cell death induced by different chemotherapeutic drugs in human leukemic T-lymphocytes. Biochem Pharmacol 1996;51:1331–40.
[39] Susin SA, Lorenzo HK, Zamzami N, Marzo I, Snow BE, Brothers GM, et al. Molecular characterization of mitochondrial apoptosis-inducing factor. Nature 1999;397:441–6.
[40] Cory S, Huang DC, Adams JM. The Bcl-2 family: roles in cell survival and oncogenesis. Oncogene 2003;22:8590–607.
[41] Golsteyn RM. Cdk1 and Cdk2 complexes (cyclin dependent kinases) in apoptosis: a role beyond the cell cycle. Cancer Lett 2005;217:129–38.
[42] Bunz F, Dutriaux A, Lengauer C, Waldman T, Zhou S, Brown JP, et al. Requirement for p53 and p21 to sustain G2 arrest after DNA damage. Science 1998;282:1497–501.
[43] Sankala HM, Hait NC, Paugh SW, Shida D, Lepine S, Elmore LW, et al. Involvement of sphingosine kinase 2 in p53-independent induction of p21 by the chemotherapeutic drug doxorubicin. Cancer Res 2007;67:10466–10474.
[44] Chang BD, Swift ME, Shen M, Fang J, Broude EV, Roninson IB. Molecular determinants of terminal growth arrest induced in tumor cells by a chemotherapeutic agent. Proc Natl Acad Sci USA 2002;99:389–94.